Applied Physics Letters

RESEARCH ARTICLE | FEBRUARY 21 2023

Si doping of β-Ga_2O_3 by disilane via hybrid plasma-assisted molecular beam epitaxy

Zhuoqun Wen ; Kamruzzaman Khan ; Xin Zhai ; Elaheh Ahmadi

Appl. Phys. Lett. 122, 082101 (2023)
https://doi.org/10.1063/5.0142107

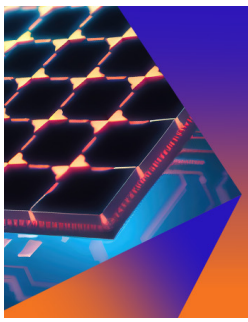

Applied Physics Letters ARTICLE scitation.org/journal/apl

Si doping of β-Ga_2O_3 by disilane via hybrid plasma-assisted molecular beam epitaxy

Cite as: Appl. Phys. Lett. **122**, 082101 (2023); doi: 10.1063/5.0142107
Submitted: 11 January 2023 · Accepted: 5 February 2023 ·
Published Online: 21 February 2023

View Online Export Citation CrossMark

Zhuoqun Wen,[1,a)] Kamruzzaman Khan,[1] Xin Zhai,[2] and Elaheh Ahmadi[2,3]

AFFILIATIONS

[1]Department of Materials Science and Engineering, University of Michigan, Ann Arbor, Michigan 48109, USA
[2]Department of Electrical Engineering and Computer Science, University of Michigan, Ann Arbor, Michigan 48109, USA
[3]Applied Physics Program, University of Michigan, Ann Arbor, Michigan 48109, USA

[a)]Author to whom correspondence should be addressed: wzhuoqun@umich.edu

ABSTRACT

Obtaining uniform silicon concentration, especially with low concentrations (ranging from 1×10^{16} to 1×10^{18} cm^{-3}) by molecular beam epitaxy, has been challenging due to oxidation of a silicon solid source in the oxide environment. In this work, Si doping of β-Ga_2O_3 (010) films by diluted disilane as the Si source is investigated using hybrid plasma-assisted molecular beam epitaxy. The impact of growth temperature, disilane source concentration, and disilane flow rate on Si incorporation was studied by secondary ion mass spectrometry. Uniform Si concentrations ranging from 3×10^{16} to 2×10^{19} cm^{-3} are demonstrated. Si-doped β-Ga_2O_3 films with different silicon concentrations were grown on Fe-doped β-Ga_2O_3 (010) substrates. The electron concentration and mobility were determined using van de Pauw Hall measurements. A high mobility of 135 $cm^2/V\,s$ was measured for an electron concentration of 3.4×10^{17} cm^{-3} at room temperature.

In recent years, β-Ga_2O_3 due to the ultra-wide bandgap (4.8 eV) has attracted a great deal of interest as a promising candidate for the next generation of power electronics, solar-blind ultra-violet (UV) detectors, and as a substrate for UV light emitting diodes (LEDs).[1–6] Baliga's figure of merit (BFOM) of Ga_2O_3 is larger than other common wide bandgap materials such as SiC and GaN.[7] The availability of large-scale substrates and good thermal stability of β-Ga_2O_3 facilitate the development of β-Ga_2O_3 devices as well.[3,8] Different lateral and vertical β-Ga_2O_3 diodes and transistors, such as Schottky barrier diodes (SBDs),[9–16] metal-oxide-semiconductor field-effect transistors (MOSFETs),[9,17–21] Fin field-effect transistors (FinFETs),[22–26] modulation-doped field-effect transistors (MODFETs),[27–29] and current aperture vertical electron transistors (CAVETs),[30–32] have been demonstrated.

In order to realize or further improve the aforementioned devices, it is of essential importance to have the ability to grow high-quality β-Ga_2O_3 thin films with controlled doping concentrations over a wide range. N-type doping of β-Ga_2O_3 has been achieved using Sn, Si, and Ge by metal-organic chemical vapor deposition (MOCVD),[33–37] pulsed laser deposition (PLD),[38] and molecular beam epitaxy (MBE), respectively.[39–44] Nevertheless, in conventional MBE systems, achieving Si-doped β-Ga_2O_3 films with a wide range of doping concentrations and uniform doping profiles, especially at lower doping concentrations (1×10^{16}–1×10^{18} cm^{-3}) has been challenging due to oxidation of solid Si in the oxygen-rich environment.[40] Recently, McCandless *et al.*[41] achieved Si doping ranging from 1×10^{17} cm^{-3} Si to 1×10^{20} cm^{-3} in plasma-assisted molecular beam epitaxy (PAMBE) by inserting an endplate into the Si crucible to prevent oxidation of the silicon solid source. A peak room temperature mobility of 129 $cm^2/V\,s$ with a carrier concentration of 1.07×10^{17} cm^{-3} was demonstrated.

We propose Si doping using diluted disilane as a gas source in a hybrid MBE system. In the past, disilane had been used in MBE for epitaxial growth of Si[45,46] as well as Si doping of (Al, Ga)As.[47–49] The carrier concentrations between 10^{17} and 10^{18} cm^{-3} have been achieved in GaAs using disilane via MBE.[47] Compared with other organometallic precursors for Si, such as silane (SiH_4) and triethylsilane [$(C_2H_5)_3SiH$], diluted disilane is less hazardous, not flammable, easier to handle, and has no C-H bond, which would typically lead to unintentional carbon incorporation.[50]

In this work, we have used diluted disilane (Si_2H_6/N_2) to obtain Si-doped β-Ga_2O_3 by hybrid MBE. The impact of growth temperature (T_c), disilane concentration [0.01 weight percentage (wt. %) vs 10 wt. %], and disilane flow rate ($Q_{disilane}$) on silicon incorporation, carrier density, and mobility are investigated. Atomic force microscopy (AFM) was used to characterize surface morphology of films. Secondary ion mass

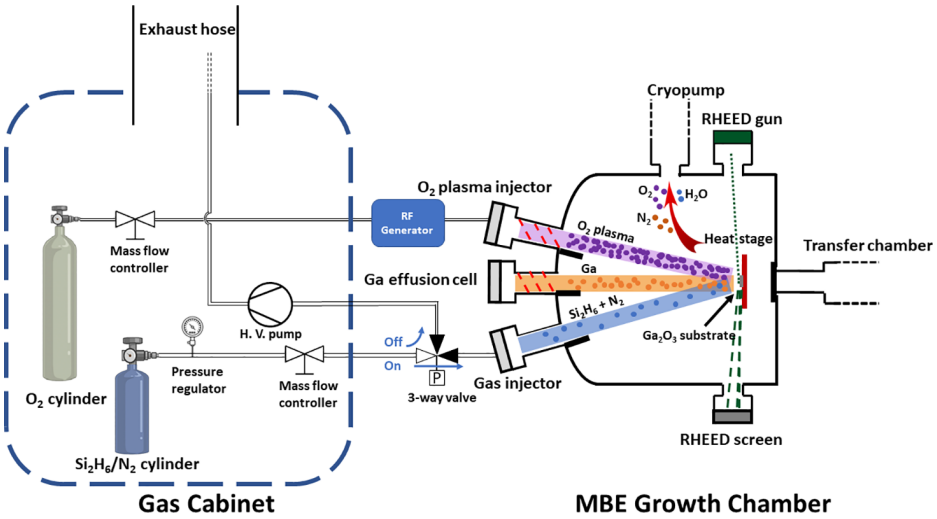

FIG. 1. Schematic of the hybrid MBE system. The diluted disilane cylinder is placed in a gas cabinet equipped with gas detectors for safety. A pressure regulator is directly connected to the disilane cylinder. $Q_{disilane}$ is controlled by an MFC. The disilane gas line is controlled by a normally off three-way pneumatic valve prior to the gas injector. At off-state, the disilane flow is directed to the exhaust line, and the excess disilane existing in the gas line is pumped out by the high vacuum pumping system. During the growth, the three-way valve is set into on-state, and the diluted disilane is delivered into the growth chamber.

spectroscopy (SIMS) was utilized to determine the Si concentration and doping profile. The room temperature carrier concentration and mobility of Si-doped β-Ga_2O_3 films were determined by van der Pauw Hall measurement.

All samples were grown in a RIBER 32 hybrid MBE system equipped with conventional Ga effusion and Ge thermal effusion cells. The oxygen source consisted of ultra-high purified oxygen (>99.999%) and was activated by the RIBER RF-O 50/63 oxygen RF plasma source. A plasma power and an oxygen flow rate of 410 W and 2 sccm, respectively, and a Ga flux of 10^{-8} Torr were used for all growths presented here, which is corresponding to a growth rate of 110 nm/h. Diluted disilane was supplied via a custom-built gas delivery system. Disilane was diluted by N_2 gas. Two different disilane concentrations were used in our studies, including 0.01 and 10 wt. %. The gas delivery system included an APtech 1410 T pressure regulator with two Swagelok PGU-50-P300-L-4FSF ultrahigh-purity pressure gauges, a calibrated Bronkhorst MFC, and a customized three-way pneumatic valve, consisted of two normally closed pneumatic valves APtech AP3540s and AP4540s. $Q_{disilane}$ was controlled by MFC. The flow rate range for 0.01 and 10 wt. % disilane was 0–0.705 and 0–0.588 sccm, respectively. In the idle state, the disilane valve was closed, the output pressure was set to zero by the pressure regulator, and the three-way valve was set to "off-state." A schematic of our hybrid MBE system is shown in Fig. 1. (The Ge cell is not shown to save space.)

Fe-doped, semi-insulating, bulk β-Ga_2O_3 (010) substrates were used in our studies. A 500 nm Ti layer was deposited on the backside of the substrates for better heat transfer as well as better adhesion to the silicon wafer via In-bonding. The substrates were first diced into $5 \times 5\,mm^2$ or $5 \times 10\,mm^2$ pieces and after solvent-cleaning were indium-bonded to 3-in. Si wafers before being transferred into the growth chamber.

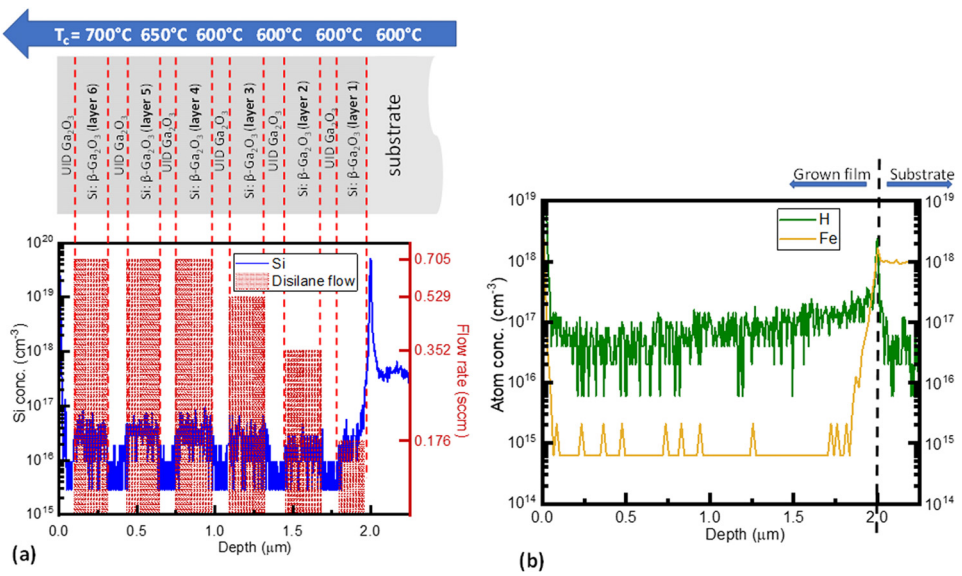

FIG. 2. (a) Schematic of the epi-layer grown for SIMS. The Si profile in β-Ga_2O_3 doped with 0.01 wt. % diluted disilane at different T_c (600, 650, and 700 °C) and $Q_{disilane}$ (from 0.176 to 0.705 sccm). (b) The H profile and Fe profile measured on the same sample by SIMS.

The growth was initiated with 30 min of oxygen polishing (the oxygen flow rate and RF power of 1 sccm and 350 W, respectively) followed by 30 min of Ga etching (Ga flux at 1×10^{-8} Torr) conducted at 800 °C to remove the impurities on the substrate surface.[51,52] A 220 nm unintentionally doped (UID) buffer layer was first grown to separate the Si-doped layer from the substrate interface. It has been shown that Fe from the substrate tends to incorporate into β-Ga_2O_3 due to the surface riding effect.[53] Fe is a donor trap and compensates free electrons, leading to poor electron mobility.[54,55] Before growing the Si-doped layer, the three-way pneumatic valve in the gas delivery system was set to off-state for 15 min to pump out the excess disilane that existed in the gas lines. Then the three-way valve was turned to "on-state," and the disilane was delivered directly to the MBE growth chamber through a low-temperature gas injector cell at room temperature.

The sample surface morphology and surface roughness were studied by atomic force microscopy (AFM). Secondary ion mass spectrometry (SIMS) was utilized to measure the Si concentration and uniformity as well as unintentional incorporation of impurities such as hydrogen, iron, and carbon. The electron density and mobility of grown samples were determined by van der Pauw Hall measurements. For this purpose, indium contacts were made at four corners of each sample.

A SIMS stack was first grown using a 0.01 wt. % diluted disilane source. This SIMS stack consisted of 220 nm-thick Si-doped β-Ga_2O_3 layers separated by 110 nm-thick UID β-Ga_2O_3 layers. The growth temperature and disilane flow rate were varied for each layer to investigate the dependence of silicon concentration on T_c and $Q_{disilane}$. As shown in Fig. 2(a), only a slight change in the Si concentration, ranging from $\sim 3 \times 10^{16}$ to $\sim 6 \times 10^{16}$ cm^{-3}, was observed when $Q_{disilane}$ was varied from 0.176 to 0.705sccm. To obtain higher Si doping concentrations with enhanced controllability, the gas source was later switched to 10 wt. % diluted disilane for the rest of the samples discussed in this work. Figure 2(b) shows H and Fe profiles. The H incorporation was measured to be $\sim 1 \times 10^{17}$ cm^{-3} throughout the MBE-grown film and the substrate and did not seem to have any correlation with the disilane flow rate. A Fe tail of ~200 nm can be observed from the SIMS profile, which is expected and is due to the Fe incorporated from the substrate as explained earlier. Beyond the initial 200 nm-thick layer, the Fe concentration was at the detecting limit. The sudden jump of H, Si, and Fe at the interface is probably due to substrate surface contamination prior to the growth.[56]

To further increase the silicon incorporation, 10 wt. % diluted disilane was used. A SIMS stack was first grown at $T_c = 525$ °C, in which Si-doped layers were separated by 110 nm-thick UID Ga_2O_3 films. Si and H profiles are shown in Fig. 3. The Si concentration increased from 6×10^{17} to 2×10^{19} cm^{-3} as $Q_{disilane}$ increased from 0.024 to 0.588 sccm. The Si profile revealed sharp interfaces with a uniform doping plateau along the growth. The H concentration remained constant throughout the MBE-grown film and similar to the H concentration in the substrate ($\sim 1 \times 10^{17}$ cm^{-3}), indicating that using disilane as the silicon source did not affect unintentional incorporation of H.

The impact of growth temperature on silicon incorporation was also investigated. Figure 4 shows the Si concentrations of samples grown at different temperatures obtained by SIMS. A $Q_{disilane}$ of 0.588 sccm was used for all four samples shown in this figure. SIMS revealed a relatively sharp and uniform doping profile within the 220 nm-thick silicon doped layer for the growth temperatures ranging from 525 to 700 °C. While a similar silicon concentration of $\sim 1.8 \times 10^{19}$ cm^{-3} was

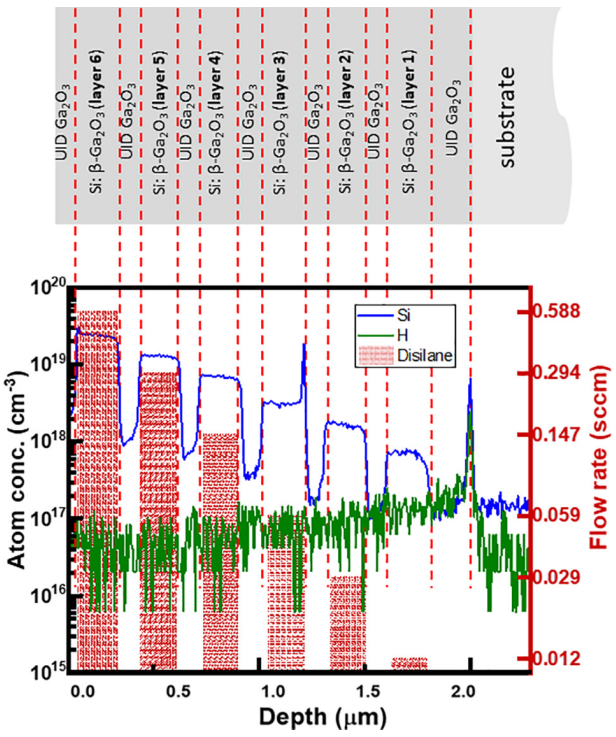

FIG. 3. Si doping profile of the Ga_2O_3 film grown at $T_c = 525$ °C varying $Q_{disilane}$ measured by SIMS. The $Q_{disilane}$ is indicated by the red dashed–dotted rectangles for each Si doped layer. 6×10^{17}–2×10^{19} cm^{-3} Si concentrations in β-Ga_2O_3 layers were obtained by changing the flow rate from 0.012 to 0.588 sccm.

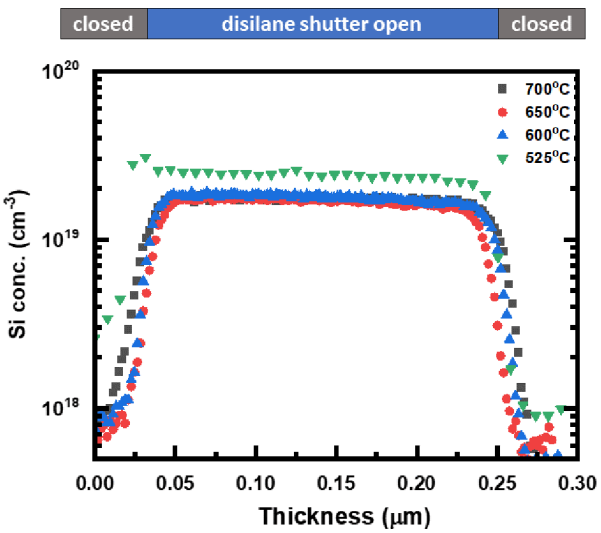

FIG. 4. Si doping profile of Ga_2O_3 grown at different temperatures, measured by SIMS. The disilane shutter was opened for 2 h with a flow rate of 0.588 sccm.

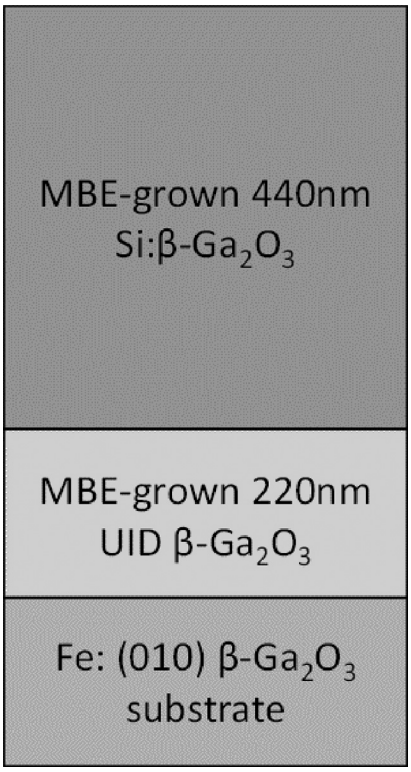

FIG. 5. Schematic of the epi-structure grown to evaluate electron transport in Si-doped Ga_2O_3 films.

measured on samples grown at $T_c = 600$, 650, and 700 °C, the Si incorporation slightly increased to 2.3×10^{19} cm^{-3} on the sample grown at 525 °C. It is worth mentioning that the growth rate remained the same (110 nm/h) for growth temperatures ranging from 525 to 700 °C.

In the next step, a series of samples with the epi-structure shown in Fig. 5 were grown at different temperatures ranging from 500 to 700 °C using 10 wt. % diluted disilane with a $Q_{disilane}$ of 0.029 sccm. A terrace-like surface morphology was observed on all samples as shown in Fig. 6. These terraces propagated along the β-Ga_2O_3 [100] direction, which is consistent with the previous reports.[57] While the samples grown at $T_c = 500$ and 525 °C showed sub-nm surface root mean square (rms) roughness, the surface rms roughness increased significantly as the growth temperature increased due to step bunching. Moreover, the length of traces increased by increasing the growth temperature. This behavior has been previously observed in other step-bunching growth regimes such as MBE-grown Si (111) and MOCVD-grown GaAs (001).[58,59]

In order to evaluate the room temperature electron concentration and mobility, Hall measurements were performed on theses samples (grown at $T_c < 650$ °C). Due to poor structural quality and high surface roughness, the samples grown at $T_c \geq 650$ °C were highly resistive and difficult to make good Ohmic contacts to. Therefore, only samples grown at $T_c = 525$–600 °C were characterized by Hall measurements. The electron mobility and density measured on these samples are reported in Table I and illustrated in Fig. 7. Carrier concentrations vs $Q_{disilane}$ at different T_c are shown in Fig. 7(a). For all growth temperatures, the carrier concentration increased as $Q_{disilane}$ increased. For the same $Q_{disilane}$, similar carrier concentrations were measured on samples grown at $T_c = 550$ and 600 °C. However, samples grown at 525 °C had slightly higher carrier concentration, which is consistent

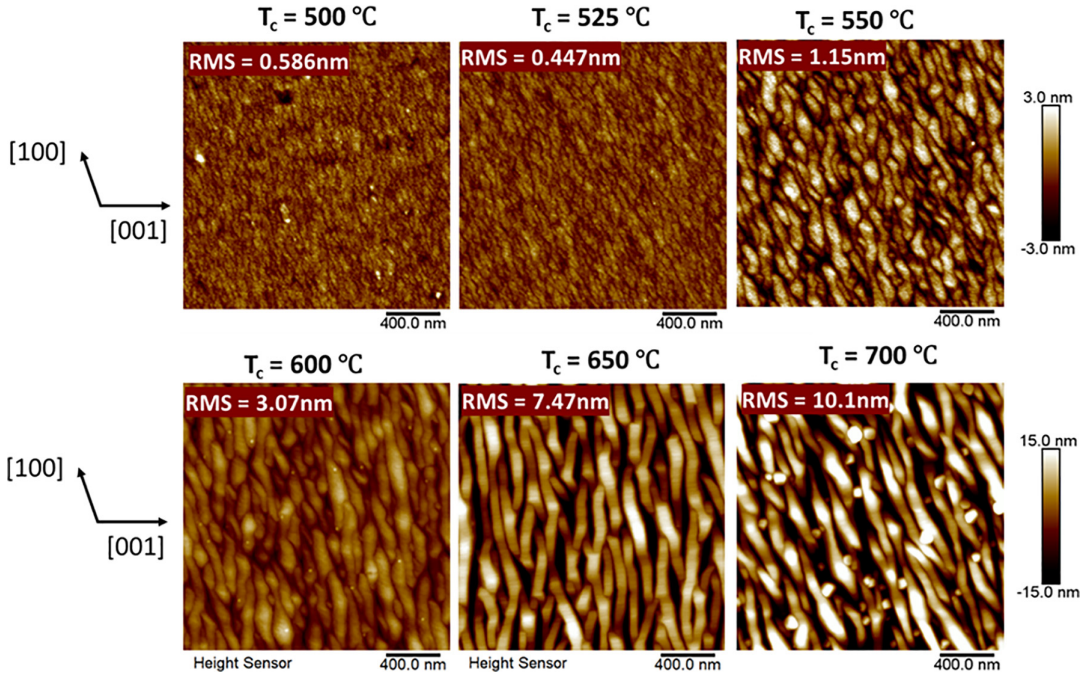

FIG. 6. 2×2 μm^2 AFM images of Si doped β-Ga_2O_3 grown with $Q_{disilane} = 0.029$ sccm at different T_c. RMS surface roughness are indicated. The height profile indication for $T_c = 500$, 525, and 550 °C is in the range of ±3.0 nm and for $T_c = 600$, 650, and 700 °C is ±15.0 nm.

TABLE I. Room temperature carrier concentration and mobility vs T_c and $Q_{disilane}$.

	$T_c = 525\,^{\circ}C$		$T_c = 550\,^{\circ}C$		$T_c = 600\,^{\circ}C$	
$Q_{disilane}$ (sccm)	Carrier concentration (cm^{-3})	Mobility ($cm^2/V\,s$)	Carrier concentration (cm^{-3})	Mobility ($cm^2/V\,s$)	Carrier concentration (cm^{-3})	Mobility ($cm^2/V\,s$)
0.012	3.4×10^{17}	135	2.1×10^{17}	100	2.0×10^{17}	20
0.029	9.6×10^{17}	88	5.8×10^{17}	65	4.5×10^{17}	33
0.059	1.7×10^{18}	83	1.2×10^{18}	62	1.1×10^{18}	79
0.147	4.3×10^{18}	45	2.5×10^{18}	60	4.5×10^{18}	38
0.294	8.1×10^{18}	30	7.7×10^{18}	55	7.0×10^{18}	48
0.588	1.8×10^{19}	20	1.4×10^{19}	34	1.1×10^{19}	66

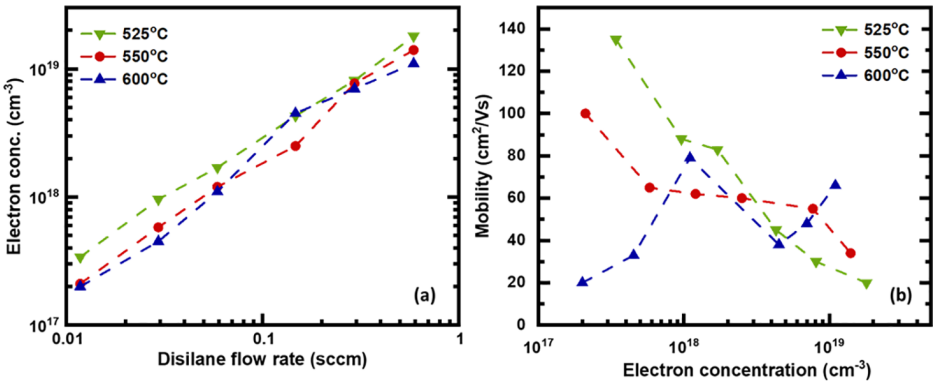

FIG. 7. (a) Hall measurement carrier concentration vs different disilane flow rates for samples grown at T_c = 525, 550, and 600 °C. (b) Hall mobility vs carrier concentration for samples grown at T_c = 525, 550, and 600 °C.

with higher silicon incorporation as observed in the SIMS profile (Fig. 5). It is worth noting that the electron concentration in all samples is 20%–40% lower than the Si concentration. Knowing that Si is a shallow donor in β-Ga_2O_3 (E_d = 16–50 meV),[60] a lower carrier concentration than the Si concentration suggests the existence of compensating centers in the film. Nitrogen could be one of the compensating centers as it is a deep acceptor trap in Ga_2O_3. SIMS analysis on our samples revealed $\sim 1 \times 10^{17} cm^{-3}$ unintentional incorporation of nitrogen in the grown films. This level of N unintentional incorporation in Ga_2O_3 has been previously reported in other MBE grown films.[61] However, this does not fully explain the difference between the Si density and electron concentration observed in our samples. Other possible compensating centers could be due to point defects formed by either high plasma power or background impurities that lead to deep acceptor levels in β-Ga_2O_3. The carrier mobilities are shown in Fig. 7(b). The electron mobility reduced as the electron density increased for samples grown at T_c = 525 and 550 °C. This is expected and is due to more ionized impurity scattering in samples with higher doping concentrations. In contrast, for samples grown at 600 °C, the electron mobility did not follow a monotonic trend with an increase in the electron concentration. This non-monotonic behavior could be explained by defect-related compensating centers generated because of high growth temperature. The electron mobility on samples with lower electron density is limited by scattering from such compensating centers. Therefore, higher electron density can help in screening these scattering centers and leads to enhanced electron mobility. However, as the doping concentration increases further, the mobility becomes limited by the ionized impurity scattering and, therefore, reduces as the doping concentration increases. Figure 8 summarizes the mobility vs electron concentration reported for Si, Ge and Sn dopants of β-Ga_2O_3 (010) by different growth techniques. The black bold squares represent our data points. The sample grown at T_c = 525 °C and $Q_{disilane}$ = 0.012 sccm showed a record room temperature mobility of 135 $cm^2/V\,s$ at a carrier density of $3.4 \times 10^{17} cm^{-3}$.

In summary, we reported Si doping of β-Ga_2O_3 (010) using diluted disilane as the Si source in the hybrid-PAMBE. The Si incorporation into β-Ga_2O_3 films as a function of the growth temperature, disilane source concentration, and disilane flow rate was investigated.

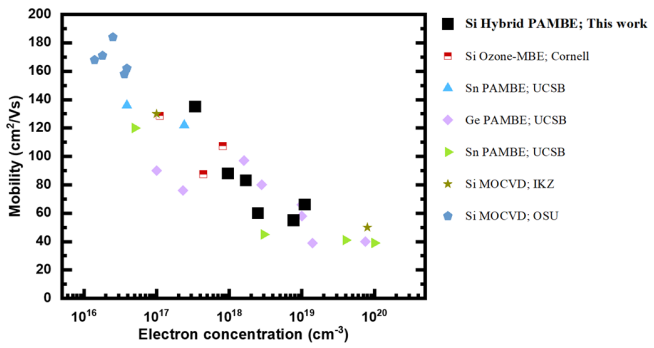

FIG. 8. The summary of the reported mobility vs electron concentration for different dopants of β-Ga_2O_3 (010) by various growth techniques.

Our studies revealed that for the growth temperature ranging from 550 to 700 °C, Si incorporation did not depend on the growth temperature, whereas the Si incorporation increased slightly at $T_c = 525$ °C. Moreover, we showed that unintentional incorporation of H was not affected by using diluted disilane as the Si source. A wide range of Si doping concentrations (1×10^{16}–2×10^{19} cm^{-3}) with uniform profile was obtained. An electron mobility of 135 $cm^2/V\,s$ was measured for an electron concentration of $3.4 \times 10^{17} cm^{-3}$. Our studies demonstrate that diluted disilane is promising as the Si source for growing Si-doped β-Ga_2O_3 by MBE.

This work was supported by the Air Force Office of Scientific Research (Program Manager, Dr. Ali Sayir) through Program No. FA9550-20-1-0045, the National Science Foundation under Grant No. 2043803, and DARPA under Grant No. N660012214032. The authors also thank Dennis Schweiger at Lurie Nanofabrication Facility of the University of Michigan for helping with building the gas delivery system.

AUTHOR DECLARATIONS

Conflict of Interest

The authors have no conflicts to disclose.

Author Contributions

Zhuoqun Wen: Conceptualization (equal); Data curation (lead); Investigation (lead); Methodology (lead); Visualization (lead); Writing – original draft (lead); Writing – review & editing (equal). **Kamruzzaman Khan:** Data curation (equal); Investigation (equal); Methodology (equal); Writing – review & editing (equal). **Xin Zhai:** Investigation (equal); Writing – review & editing (equal). **Elaheh Ahmadi:** Conceptualization (lead); Funding acquisition (lead); Investigation (equal); Methodology (equal); Writing – original draft (equal); Writing – review & editing (equal).

DATA AVAILABILITY

The data that support the findings of this study are available from the corresponding author upon reasonable request.

REFERENCES

[1]H. H. Tippins, "Optical absorption and photoconductivity in the band edge of β-Ga_2O_3," Phys. Rev. **140**(1A), A316 (1965).
[2]J. Zhang, J. Shi, D.-C. Qi, L. Chen, and K. H. Zhang, "Recent progress on the electronic structure, defect, and doping properties of Ga_2O_3," APL Mater. **8**(2), 020906 (2020).
[3]S. Stepanov, V. Nikolaev, V. Bougrov, and A. Romanov, "Gallium OXIDE: Properties and application - a review," Rev. Adv. Mater. Sci. **44**, 63 (2016).
[4]R. Suzuki, S. Nakagomi, Y. Kokubun, N. Arai, and S. Ohira, "Enhancement of responsivity in solar-blind β-Ga_2O_3 photodiodes with a Au Schottky contact fabricated on single crystal substrates by annealing," Appl. Phys. Lett. **94**(22), 222102 (2009).
[5]M. Orita, H. Ohta, M. Hirano, and H. Hosono, "Deep-ultraviolet transparent conductive β-Ga_2O_3 thin films," Appl. Phys. Lett. **77**(25), 4166 (2000).
[6]D. Guo, Z. Wu, P. Li, Y. An, H. Liu, X. Guo, H. Yan, G. Wang, C. Sun, and L. Li, "Fabrication of β-Ga_2O_3 thin films and solar-blind photodetectors by laser MBE technology," Opt. Mater. Express **4**(5), 1067 (2014).
[7]B. Jayant Baliga, "Semiconductors for high-voltage, vertical channel field-effect transistors," J. Appl. Phys. **53**(3), 1759 (1982).
[8]A. Kuramata, K. Koshi, S. Watanabe, Y. Yamaoka, T. Masui, and S. Yamakoshi, "High-quality β-Ga_2O_3 single crystals grown by edge-defined film-fed growth," Jpn. J. Appl. Phys. **55**(12), 1202A2 (2016).
[9]S. J. Pearton, F. Ren, M. Tadjer, and J. Kim, "Perspective: Ga_2O_3 for ultra-high power rectifiers and MOSFETS," J. Appl. Phys. **124**(22), 220901 (2018).
[10]M. Higashiwaki, K. Konishi, K. Sasaki, K. Goto, K. Nomura, Q. Tu Thieu, R. Togashi, H. Murakami, Y. Kumagai, and B. Monemar, "Temperature-dependent capacitance–voltage and current–voltage characteristics of Pt/Ga_2O_3 (001) Schottky barrier diodes fabricated on n-Ga2O3 drift layers grown by halide vapor phase epitaxy," Appl. Phys. Lett. **108**(13), 133503 (2016).
[11]Z. Hu, K. Nomoto, W. Li, Z. Zhang, N. Tanen, Q. Tu Thieu, K. Sasaki, A. Kuramata, T. Nakamura, and D. Jena, "Breakdown mechanism in 1 kA/cm^2 and 960 V E-mode β-Ga_2O_3 vertical transistors," Appl. Phys. Lett. **113**(12), 122103 (2018).
[12]J. Yang, F. Ren, M. Tadjer, S. J. Pearton, and A. Kuramata, "2300 V reverse breakdown voltage Ga_2O_3 Schottky rectifiers," ECS J. Solid State Sci. Technol. **7**(5), Q92 (2018).
[13]K. Konishi, K. Goto, H. Murakami, Y. Kumagai, A. Kuramata, S. Yamakoshi, and M. Higashiwaki, "1-kV vertical Ga_2O_3 field-plated Schottky barrier diodes," Appl. Phys. Lett. **110**(10), 103506 (2017).
[14]L. Du, Q. Xin, M. Xu, Y. Liu, W. Mu, S. Yan, X. Wang, G. Xin, Z. Jia, and X.-T. Tao, "High-performance Ga_2O_3 diode based on tin oxide Schottky contact," IEEE Electron Device Lett. **40**(3), 451 (2019).
[15]L. Du, Q. Xin, M. Xu, Y. Liu, G. Liang, W. Mu, Z. Jia, X. Wang, G. Xin, and X.-T. Tao, "Achieving high performance Ga_2O_3 diodes by adjusting chemical composition of tin oxide Schottky electrode," Semicond. Sci. Technol. **34**(7), 075001 (2019).
[16]C. Joishi, S. Rafique, Z. Xia, L. Han, S. Krishnamoorthy, Y. Zhang, S. Lodha, H. Zhao, and S. Rajan, "Low-pressure CVD-grown β-Ga_2O_3 bevel-field-plated Schottky barrier diodes," Appl. Phys. Express **11**(3), 031101 (2018).
[17]K. Zeng, Y. Jia, and U. Singisetti, "Interface state density in atomic layer deposited SiO_2/β-Ga_2O_3 MOSCAPs," IEEE Electron Device Lett. **37**(7), 906 (2016).
[18]M. A. Bhuiyan, H. Zhou, R. Jiang, E. X. Zhang, D. M. Fleetwood, D. Ye Peide, and T.-P. Ma, "Charge trapping in Al_2O_3/β-Ga_2O_3-based MOS capacitors," IEEE Electron Device Lett. **39**(7), 1022 (2018).
[19]H. Bae, J. Noh, S. Alghamdi, M. Si, and D. Ye Peide, "Ultraviolet light-based current–voltage method for simultaneous extraction of donor-and acceptor-like interface traps in β-Ga_2O_3 FETs," IEEE Electron Device Lett. **39**(11), 1708 (2018).
[20]M. Hoi Wong, K. Sasaki, A. Kuramata, S. Yamakoshi, and M. Higashiwaki, "Field-plated Ga_2O_3 MOSFETs with a breakdown voltage of over 750 V," IEEE Electron Device Lett. **37**(2), 212 (2016).
[21]M. Higashiwaki, K. Sasaki, A. Kuramata, T. Masui, and S. Yamakoshi, "Gallium oxide (Ga_2O_3) metal-semiconductor field-effect transistors on single-crystal β-Ga_2O_3 (010) substrates," Appl. Phys. Lett. **100**(1), 013504 (2012).
[22]Z. Hu, K. Nomoto, W. Li, N. Tanen, K. Sasaki, A. Kuramata, T. Nakamura, D. Jena, and H. G. Xing, "Enhancement-mode Ga_2O_3 vertical transistors with breakdown voltage > 1 kV," IEEE Electron Device Lett. **39**(6), 869 (2018).
[23]B. Chatterjee, W. Li, K. Nomoto, H. G. Xing, and S. Choi, "Thermal design of multi-fin Ga_2O_3 vertical transistors," Appl. Phys. Lett. **119**(10), 103502 (2021).
[24]H.-C. Huang, Z. Ren, A. F. M. Anhar Uddin Bhuiyan, Z. Feng, Z. Yang, X. Luo, A. Q. Huang, A. Green, K. Chabak, and H. Zhao, "β-Ga_2O_3 FinFETs with ultra-low hysteresis by plasma-free metal-assisted chemical etching," Appl. Phys. Lett. **121**(5), 052102 (2022).
[25]S. Xu, L. Liu, G. Qu, X. Zhang, C. Jia, S. Wu, Y. Ma, Y. J. Lee, G. Wang, and J.-H. Park, "Single β-Ga_2O_3 nanowire based lateral FinFET on Si," Appl. Phys. Lett. **120**(15), 153501 (2022).
[26]Z. Hu, K. Nomoto, W. Li, R. Jinno, T. Nakamura, D. Jena, and H. Xing, paper presented at the 2019 31st International Symposium on Power Semiconductor Devices and ICs (ISPSD), Shanghai, China, May 19–23 (2019).
[27]Y. Zhang, A. Neal, Z. Xia, C. Joishi, J. M. Johnson, Y. Zheng, S. Bajaj, M. Brenner, D. Dorsey, and K. Chabak, "Demonstration of high mobility and quantum transport in modulation-doped β-$(Al_xGa_{1-x})_2O_3$/Ga_2O_3 heterostructures," Appl. Phys. Lett. **112**(17), 173502 (2018).
[28]S. Krishnamoorthy, Z. Xia, C. Joishi, Y. Zhang, J. McGlone, J. Johnson, M. Brenner, A. R. Arehart, J. Hwang, and S. Lodha, "Modulation-doped β-$(Al_{0.2}Ga_{0.8})_2O_3$/Ga_2O_3 field-effect transistor," Appl. Phys. Lett. **111**(2), 023502 (2017).

[29]H. Yuan, J. Su, R. Guo, K. Tian, Z. Lin, J. Zhang, J. Chang, and Y. Hao, "Contact barriers modulation of graphene/β-Ga_2O_3 interface for high-performance Ga_2O_3 devices," Appl. Surf. Sci. **527**, 146740 (2020).
[30]M. Hoi Wong, K. Goto, Y. Morikawa, A. Kuramata, S. Yamakoshi, H. Murakami, Y. Kumagai, and M. Higashiwaki, "All-ion-implanted planar-gate current aperture vertical Ga_2O_3 MOSFETs with Mg-doped blocking layer," Appl. Phys. Express **11**(6), 064102 (2018).
[31]M. Hoi Wong, K. Goto, H. Murakami, Y. Kumagai, and M. Higashiwaki, "Current aperture vertical β-Ga_2O_3 MOSFETs fabricated by N-and Si-ion implantation doping," IEEE Electron Device Lett. **40**(3), 431 (2019).
[32]M. Hoi Wong, H. Murakami, Y. Kumagai, and M. Higashiwaki, "Enhancement-mode β-Ga_2O_3 current aperture vertical MOSFETs with N-ion-implanted blocker," IEEE Electron Device Lett. **41**(2), 296 (2020).
[33]F. Alema, Y. Zhang, A. Osinsky, N. Valente, A. Mauze, T. Itoh, and J. S. Speck, "Low temperature electron mobility exceeding 104 cm^2/V s in MOCVD grown β-Ga_2O_3," APL Mater. **7**(12), 121110 (2019).
[34]Z. Feng, A. F. M. A. U. Bhuiyan, M. R. Karim, and H. Zhao, "MOCVD homoepitaxy of Si-doped (010) β-Ga_2O_3 thin films with superior transport properties," Appl. Phys. Lett. **114**(25), 250601 (2019).
[35]Y. Zhang, F. Alema, A. Mauze, O. S. Koksaldi, R. Miller, A. Osinsky, and J. S. Speck, "MOCVD grown epitaxial β-Ga_2O_3 thin film with an electron mobility of 176 cm^2/V s at room temperature," APL Mater. **7**(2), 022506 (2019).
[36]M. Baldini, M. Albrecht, A. Fiedler, K. Irmscher, D. Klimm, R. Schewski, and G. Wagner, "Semiconducting Sn-doped β-Ga_2O_3 homoepitaxial layers grown by metal organic vapour-phase epitaxy," J. Mater. Sci. **51**(7), 3650 (2016).
[37]M. Baldini, M. Albrecht, A. Fiedler, K. Irmscher, R. Schewski, and G. Wagner, "Si-and Sn-doped homoepitaxial β-Ga_2O_3 layers grown by MOVPE on (010)-oriented substrates," ECS J. Solid State Sci. Technol. **6**(2), Q3040 (2017).
[38]K. D. Leedy, K. D. Chabak, V. Vasilyev, D. C. Look, J. J. Boeckl, J. L. Brown, S. E. Tetlak, A. J. Green, N. A. Moser, and A. Crespo, "Highly conductive homoepitaxial Si-doped Ga_2O_3 films on (010) β-Ga_2O_3 by pulsed laser deposition," Appl. Phys. Lett. **111**(1), 012103 (2017).
[39]E. Ahmadi, O. S. Koksaldi, S. W. Kaun, Y. Oshima, D. B. Short, U. K. Mishra, and J. S. Speck, "Ge doping of β-Ga_2O_3 films grown by plasma-assisted molecular beam epitaxy," Appl. Phys. Express **10**(4), 041102 (2017).
[40]N. K. Kalarickal, Z. Xia, J. McGlone, S. Krishnamoorthy, W. Moore, M. Brenner, A. R. Arehart, S. A. Ringel, and S. Rajan, "Mechanism of Si doping in plasma assisted MBE growth of β-Ga_2O_3," Appl. Phys. Lett. **115**(15), 152106 (2019).
[41]J. P. McCandless, V. Protasenko, B. W. Morell, E. Steinbrunner, A. T. Neal, N. Tanen, Y. Cho, T. J. Asel, S. Mou, and P. Vogt, "Controlled Si doping of β-Ga_2O_3 by molecular beam epitaxy," Appl. Phys. Lett. **121**, 072108 (2022).
[42]H. Okumura, M. Kita, K. Sasaki, A. Kuramata, M. Higashiwaki, and J. S. Speck, "Systematic investigation of the growth rate of β-Ga_2O_3 (010) by plasma-assisted molecular beam epitaxy," Appl. Phys. Express **7**(9), 095501 (2014).
[43]S.-H. Han, A. Mauze, E. Ahmadi, T. Mates, Y. Oshima, and J. S. Speck, "n-type dopants in (001) β-Ga_2O_3 grown on (001) β-Ga_2O_3 substrates by plasma-assisted molecular beam epitaxy," Semicond. Sci. Technol. **33**(4), 045001 (2018).
[44]A. Mauze, Y. Zhang, T. Itoh, E. Ahmadi, and J. S. Speck, "Sn doping of (010) β-Ga_2O_3 films grown by plasma-assisted molecular beam epitaxy," Appl. Phys. Lett. **117**(22), 222102 (2020).
[45]H. Hirayama, T. Tatsumi, and N. Aizaki, "Disilane gas source Si-MBE," J. Cryst. Growth **95**(1–4), 476 (1989).
[46]W. K. Liu, S. M. Mokler, N. Ohtani, C. Roberts, and B. A. Joyce, "A RHEED study of the surface reconstructions of Si (001) during gas source MBE using disilane," Surf. Sci. **264**(3), 301 (1992).
[47]K. Kimura, S. Horiguchi, K. Kamon, M. Shimazu, M. Mashita, M. Mihara, and M. Ishii, "Silicon doping from disilane in gas source MBE of GaAs," J. Cryst. Growth **81**(1–4), 276 (1987).
[48]A. Sandhu, T. Fujii, H. Ando, T. Takahashi, H. Ishikawa, N. O. N. Okamoto, and N. Y. N. Yokoyama, "Gas source MBE growth of GaAs/AlGaAs heterojunction bipolar transistor with a carbon doped base using only gaseous sources," Jpn. J. Appl. Phys. **30**(3R), 464 (1991).
[49]A. Sandhu, T. Fujii, H. Ando, and H. Ishikawa, "A study of cold dopant sources for gas source MBE: The use of disilane as an n-type dopant of $Al_xGa_{1-x}As$ (x = 0–0.28) and trimethylgallium as a p-type dopant of GaAs," Jpn. J. Appl. Phys. **29**(7A), L1033 (1990).
[50]M. Weyers, J. Musolf, D. Marx, A. Kohl, and P. Balk, "Gaseous dopant sources in MOMBE/CBE," J. Crystal Growth **105**(1–4), 383 (1990).
[51]Y. Oshima, E. Ahmadi, S. Kaun, F. Wu, and J. S. Speck, "Growth and etching characteristics of (001) β-Ga_2O_3 by plasma-assisted molecular beam epitaxy," Semicond. Sci. Technol. **33**(1), 015013 (2018).
[52]E. Ahmadi, Y. Oshima, F. Wu, and J. S. Speck, "Schottky barrier height of Ni to β-$(Al_xGa_{1-x})_2O_3$ with different compositions grown by plasma-assisted molecular beam epitaxy," Semicond. Sci. Technol. **32**(3), 035004 (2017).
[53]A. Mauze, Y. Zhang, T. Mates, F. Wu, and J. S. Speck, "Investigation of unintentional Fe incorporation in (010) β-Ga_2O_3 films grown by plasma-assisted molecular beam epitaxy," Appl. Phys. Lett. **115**(5), 052102 (2019).
[54]J. F. McGlone, Z. Xia, Y. Zhang, C. Joishi, S. Lodha, S. Rajan, S. A. Ringel, and A. R. Arehart, "Trapping effects in Si δ-doped β-Ga_2O_3 MESFETs on an Fe-doped β-Ga_2O_3 substrate," IEEE Electron Device Lett. **39**(7), 1042 (2018).
[55]C. Joishi, Z. Xia, J. McGlone, Y. Zhang, A. R. Arehart, S. Ringel, S. Lodha, and S. Rajan, "Effect of buffer iron doping on delta-doped β-Ga_2O_3 metal semiconductor field effect transistors," Appl. Phys. Lett. **113**(12), 123501 (2018).
[56]M. H. Wong, K. Sasaki, A. Kuramata, S. Yamakoshi, and M. Higashiwaki, "Electron channel mobility in silicon-doped Ga_2O_3 MOSFETs with a resistive buffer layer," Jpn. J. Appl. Phys. **55**(12), 1202B9 (2016).
[57]K. Sasaki, M. Higashiwaki, A. Kuramata, T. Masui, and S. Yamakoshi, "Growth temperature dependences of structural and electrical properties of Ga_2O_3 epitaxial films grown on β-Ga_2O_3 (010) substrates by molecular beam epitaxy," J. Cryst. Growth **392**, 30 (2014).
[58]H. Omi, Y. Homma, V. Tonchev, and A. Pimpinelli, "New types of unstable step-flow growth on Si (111)−(7 × 7) during molecular beam epitaxy: Scaling and universality," Phys. Rev. Lett. **95**(21), 216101 (2005).
[59]M. Shinohara and N. Inoue, "Behavior and mechanism of step bunching during metalorganic vapor phase epitaxy of GaAs," Appl. Phys. Lett. **66**(15), 1936 (1995).
[60]A. T. Neal, S. Mou, S. Rafique, H. Zhao, E. Ahmadi, J. S. Speck, K. T. Stevens, J. D. Blevins, D. B. Thomson, and N. Moser, "Donors and deep acceptors in β-Ga_2O_3," Appl. Phys. Lett. **113**(6), 062101 (2018).
[61]J. Wei, F. Liu, X. Rong, T. Wang, L. Yang, R. Tao, J. Yang, L. Guo, B. Shen, and X. Wang, "Effect of unintentional nitrogen incorporation on n-type doping of β-Ga_2O_3 grown by molecular beam epitaxy," CrystEngComm. **24**(2), 269–274 (2022).